Electronic Supplementary Material (ESI) for CrystEngComm.
This journal is © The Royal Society of Chemistry 2017

Supplementary Information

Built-in TTF-TCNQ charge-transfer salts in π-stacked pillared layer frameworks

Yoshihiro Sekine,[a,b] Masanori Tonouchi,[c] Taiga Yokoyama,[b] Wataru Kosaka[a,b] and Hitoshi Miyasaka*[,a,b]

[a] Institute for Materials Research, Tohoku University, 2-1-1 Katahira, Aoba-ku, Sendai 980-8577, Japan

[b] Department of Chemistry, Graduate School of Science, Tohoku University, 6-3 Aramaki-Aza-Aoba, Aoba-ku, Sendai 980-8578, Japan

[c] Department of Chemistry, Division of Material Sciences, Graduate School of Natural Science and Technology, Kanazawa University, Kakuma-machi, Kanazawa 920-1192, Japan

Corresponding author*

Prof. Dr. Hitoshi Miyasaka

Institute for Materials Research, Tohoku University

2–1–1 Katahira, Aoba-ku, Sendai 980-8577, Japan

E-mail: miyasaka@imr.tohoku.ac.jp

Tel: +81-22-215-2030

Fax: +81-22-215-2031

Experimental Section

General Procedures and Materials: All synthetic procedures were performed in the absence of oxygen using standard Schlenk-line techniques and a commercial glove box. All chemicals were purchased from commercial sources and were of reagent grade. Solvents were dried using common drying agents and distilled with ultrapure nitrogen prior to use. The starting materials $[Rh_2(CH_3CO_2)_4(MeOH)_2]$, $[Rh_2(o\text{-}ClPhCO_2)_4(THF)_2]$, and TTF-TCNQ were prepared according to previously reported methods.[1]

Preparation of (TTF)[{$Rh_2^{II,II}(CH_3CO_2)_4$}$_2$TCNQ]·6CH_2Cl_2 (1). A solution in dichloromethane (30 mL) of TTF-TCNQ (6.2 mg, 0.015 mmol) was separated into aliquots of 2.5 mL, which were placed in sealed glass tubes with a narrow diameter (ϕ = 8 mm) as the bottom layer. A solution in 1,2-dichloroethane (DCE) (30 mL) of $[Rh_2(CH_3CO_2)_4(MeOH)_2]$ (15.2 mg, 0.03 mmol) was carefully placed in an aliquot of 2.5 mL onto the bottom layer to allow slow diffusion to occur. The glass tubes were turned upside down and left undisturbed in a refrigerator for a few days to yield block-shaped green crystals of **1**. Yield: 21%. Elemental analysis (%) calculated for (TTF)[{$Rh_2^{II,II}(CH_3CO_2)_4$}$_2$TCNQ]·4CH_2Cl_2, $C_{38}H_{40}Cl_8N_4O_{16}Rh_4S_4$: C 27.96, H 2.47, N 3.43; found: C 28.05, H 2.41, N 3.49. FT-IR (KBr): ν(C≡ N) 2202 cm^{-1}, ν(C=O) 1560, 1440 cm^{-1}, ν(C=C) 1506 cm^{-1}.

Preparation of (TTF)[{$Rh_2^{II,II}$(*o*-ClPhCO$_2$)$_4$}$_2$TCNQ]·2CH_2Cl_2 (2). A solution in dichloromethane (20 mL) of $[Rh_2(o\text{-}ClPhCO_2)_4(THF)_2]$ (19.4 mg, 0.02 mmol) was separated into aliquots of 2.0 mL and placed in sealed glass tubes with a narrow diameter (φ = 8 mm) as the bottom layer. A mixture of dichloromethane and DCE (1:1 v/v; 1 mL), which served as the middle layer, was carefully added to the bottom layer. A solution in DCE (20 mL) of TTF-TCNQ (4.1 mg, 0.01 mmol) was carefully placed in an aliquot of 2.0 mL onto the middle layer. The glass tubes were turned upside down and left undisturbed in a refrigerator for a few days to yield block-shaped green crystals of **2**. Yield: 59%. Elemental analysis (%) calculated for fresh sample, $C_{76}H_{44}Cl_{12}N_4O_{16}Rh_4S_4$: C 40.85, H 1.98, N 2.51;

found: C 41.09, H 2.13, N 2.78. FT-IR (KBr): ν(C≡ N) 2191 cm^{-1}, ν(C=O) 1563, 1400 cm^{-1}, ν(C=C) 1505 cm^{-1}.

Preparation of $(TTF)_2[\{Rh_2^{II,II}(o\text{-}ClPhCO_2)_4\}_2TCNQ]\cdot 1.5C_2H_4Cl_2\cdot 0.5CH_2Cl_2$ (3). A solution in dichloromethane (30 mL) of $[Rh_2(o\text{-}ClPhCO_2)_4(THF)_2]$ (29.1 mg, 0.03 mmol) was separated into aliquots of 2.0 mL and placed in sealed glass tubes with a narrow diameter (ϕ = 8 mm) as the bottom layer. A mixture of dichloromethane and DCE (1:1 v/v; 1 mL), which served as the middle layer, was carefully added to the bottom layer. A solution in DCE (30 mL) of TTF-TCNQ (6.2 mg, 0.015 mmol) and TTF (9.0 mg, 0.045 mmol) was carefully placed in an aliquot of 2.0 mL onto the middle layer. The glass tubes were turned upside down and left undisturbed in a refrigerator for a few days to yield plate-shaped black crystals of **3**. Yield: 8%. Elemental analysis (%) calculated for fresh sample, $C_{83.50}H_{51}Cl_{12}N_4O_{16}Rh_4S_8$: C 40.77, H 2.09, N 2.28; found: C 40.59, H 2.10, N 2.36. FT-IR (KBr): ν(C≡ N) 2198 cm^{-1}, ν(C=O) 1563, 1401 cm^{-1}, ν(C=C) 1505 cm^{-1}.

Crystal structural analyses: Crystal data for **1**, **2**, and **3** were collected at 93 K using a CCD diffractometer (Rigaku Saturn 70) with multi-layer mirror-monochromated Mo Kα radiation (λ = 0.71075 Å). A single crystal was mounted on a thin Kapton film with Nujol and cooled in an N_2 gas stream. The structures were solved using direct methods (SHELXL-97)[2] and expanded using Fourier techniques. Full-matrix least-squares refinement on F^2 was performed based on observed reflections and variable parameters, and the refinement cycle was estimated from unweighted and weighted agreement factors of $R1 = \Sigma||F_o| - |F_c||/\Sigma|F_o|$ ($I > 2.00\sigma(I)$ and all data) and $wR2 = [\Sigma(w(F_o^2 - F_c^2)^2)/\Sigma w(F_o^2)^2]^{1/2}$ (all data). All calculations were performed using the CrystalStructure crystallographic software package.[3]

The CIF data have been deposited at the Cambridge Crystallographic Data Centre as supplementary publication nos. CCDC–1536657, 1536656, and 1536658 for **1**, **2**, and **3**, respectively. Copies of the data can be obtained free of charge on application to the CCDC, 12 Union Road, Cambridge CB2 1EZ, U.K. (fax: (+44) 1223-336-033; e-mail: deposit@ccdc.cam.ac.uk).

Physical measurements: Infrared (IR) absorption spectra were recorded using the KBr disk method at room temperature with a JASCO FT-IR 4200 spectrophotometer. Thermogravimetric analysis was performed using a Shimadzu DTG-60H instrument under a flowing N_2 atmosphere. The sample was sealed in a quartz glass capillary with an inner diameter of 0.5 mm. The XRPD pattern with good counting statistics was measured using a RIGAKU Ultima IV diffractometer with Cu $K\alpha$ radiation (λ = 1.5418 Å). The XRPD pattern was obtained with a 0.02° step. Powder reflection spectra were recorded on pellets diluted with $BaSO_4$ using a Shimadzu UV-3150 spectrometer. Magnetic susceptibility measurements were conducted with a Quantum Design MPMS-XL SQUID magnetometer over the temperature and dc field ranges of 1.8 to 300 K and –7 to 7 T, respectively. Polycrystalline samples embedded in liquid paraffin were analyzed. The experimental data were corrected for the sample holder and liquid paraffin and for the diamagnetic contribution calculated from Pascal constants.[4]

Table S1. Crystallographic data for **1**–**3**.

	1	**2**	**3**
formula	$C_{40}H_{44}Cl_{12}N_4O_{16}Rh_4S_4$	$C_{76}H_{44}Cl_{12}N_4O_{16}Rh_4S_4$	$C_{83.50}H_{51}Cl_{12}N_4O_{16}Rh_4S_8$
formula weight	1802.1	2234.5	2459.88
crystal system	triclinic	triclinic	triclinic
space group	*P*-1 (*#2*)	*P*-1 (*#2*)	*P*-1 (*#2*)
a / Å	8.2790(6)	10.929(2)	10.4069(13)
b / Å	13.8112(11)	13.658(3)	14.095(2)
c / Å	14.0825(13)	16.296(3)	15.263(2)
α / deg	91.101(6)	71.368(9)	86.244(3)
β / deg	97.128(5)	74.864(10)	85.165(3)
γ / deg	90.515(4)	69.076(9)	85.393(4)
V / Å^3	1597.4(3)	2122.9(7)	2219.7(5)
Z	1	1	1
crystal size / mm^3	0.170 × 0.090 × 0.080	0.174 × 0.106 × 0.055	0.330 × 0.110 × 0.040
T / K	97(1)	97(1)	97(1)
D_{calc} / g·cm^{-3}	1.873	1.784	1.84
F_{000}	888	1104	1220
λ / Å	0.71075	0.71075	0.71075
μ(Mo Kα) / cm^{-1}	17.065	13.035	13.466
data measured	10531	14346	15005
data unique	5469	7282	7626
R_{int}	0.0387	0.0228	0.0209
no. of observations	5469	7282	7626
no. of variables	361	556	604
R_1 ($I > 2.00\ \sigma(I)$)[a]	0.0716	0.0514	0.0496
R (all reflections)[a]	0.0818	0.0551	0.0528
wR_2 (all reflections)[b]	0.2091	0.1398	0.1333
GOF	1.092	1.063	1.067
CCDC No.	1536657	1536656	1536658

[a] $R_1 = R = \Sigma\ ||F_o| - |F_c||/\Sigma|F_o|$, [b] $wR_2 = [\ \Sigma w(F_o^2 - F_c^2)^2)/\Sigma w(F_o^2)^2]^{1/2}$

Table S2. Selected bond lengths (Å) in **1**–**3**

	1	**2**	**3**
Rh(1)-O(1)	2.032(6)	2.044(12)	2.031(4)
Rh(1)-O(2)	2.034(6)[a]	2.036(12)[c]	2.034(4)[e]
Rh(1)-O(3)	2.038(6)	2.043(11)	2.050(4)
Rh(1)-O(4)	2.049(6)[a]	2.021(11)[c]	2.026(4)[e]
Rh(2)-O(5)	2.038(5)	2.037(11)	2.039(4)
Rh(2)-O(6)	2.039(5)[b]	2.042(11)[d]	2.053(4)[f]
Rh(2)-O(7)	2.033(6)	2.032(12)	2.033(4)
Rh(2)-O(8)	2.031(6)[b]	2.033(11)[d]	2.036(4)[f]
Rh(1)-Rh(1)	2.3916(8)[a]	2.4026(16)[c]	2.4022(5)[e]
Rh(2)-Rh(2)	2.4012(9)[b]	2.3991(12)[d]	2.204(5)[f]

* Symmetry codes: (a) −*x*, −*y*+1, −*z*, (b) −*x*, −*y*+2, −*z*+1, (c) −*x*, −*y*+2, −*z*, (d) −*x*+1, −*y*+1, −*z*+1, (e) –*x*+2, –*y*+1, –*z*+1, (f) –x+2, –*y*, –*z*+2

Table S3. Bond lengths (Å) in the TCNQ.

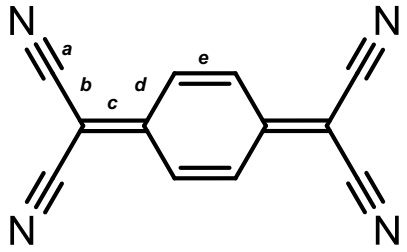

	charge	*a*	*b*	*c*	*d*	*e*	ρ^b	Ref.
I	0	1.140(1)	1.441(4)	1.374(3)	1.448(4)	1.346(3)	0	5
II	−1	1.153(7)	1.416(8)	1.420(1)	1.423(3)	1.373(1)	−1	6
1		1.173(11)	1.404(11)	1.410(11)	1.417(11)	1.374(11)	−0.87	this work
		1.137(11)	1.425(12)		1.431(10)			
		1.155[a]	1.414[a]		1.424[a]			
2		1.14(2)	1.43(2)	1.41(2)	1.420(17)	1.37(2)	−0.82	this work
		1.147(15)	1.410(16)		1.43(2)			
		1.144[a]	1.42[a]		1.425[a]			
3		1.146(7)	1.419(7)	1.423(7)	1.425(7)	1.364(7)	−1.04	this work
		1.148(7)	1.417(7)		1.421(7)			
		1.147[a]	1.418[a]		1.423[a]			

I = TCNQ, **II** = RbTCNQ, [a]average value in a molecule, [b]estimated from the average values

Table S4. Bond lengths (Å) in the TTF.

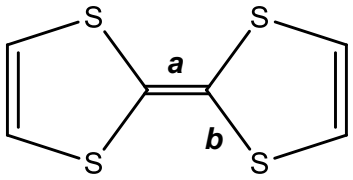

	charge	*a*	*b*	*a* / *b*	ρ^b	ref
I	0	1.349	1.757	0.768	0.13	7
II	0.59	1.369	1.743	0.785	0.48	8
III	1	1.404	1.713	0.820	1.19	9
1		1.389(14)	1.714(10) 1.721(10) 1.718[a]	0.808	0.96	this work
2		1.39(3)	1.722(19) 1.718(15) 1.720[a]	0.808	0.95	this work
3		1.366(9)	1.730(6) 1.747(6) 1.748(6) 1.739(7) 1.741[a]	0.785	0.47	this work

I = TTF, **II** = TTF-TCNQ, **III** = TTF-ClO_4, ρ = A(a/b)+B with A = 20.42, with B = −15.55, [a]average value in a molecule, [b]estimated from the average values

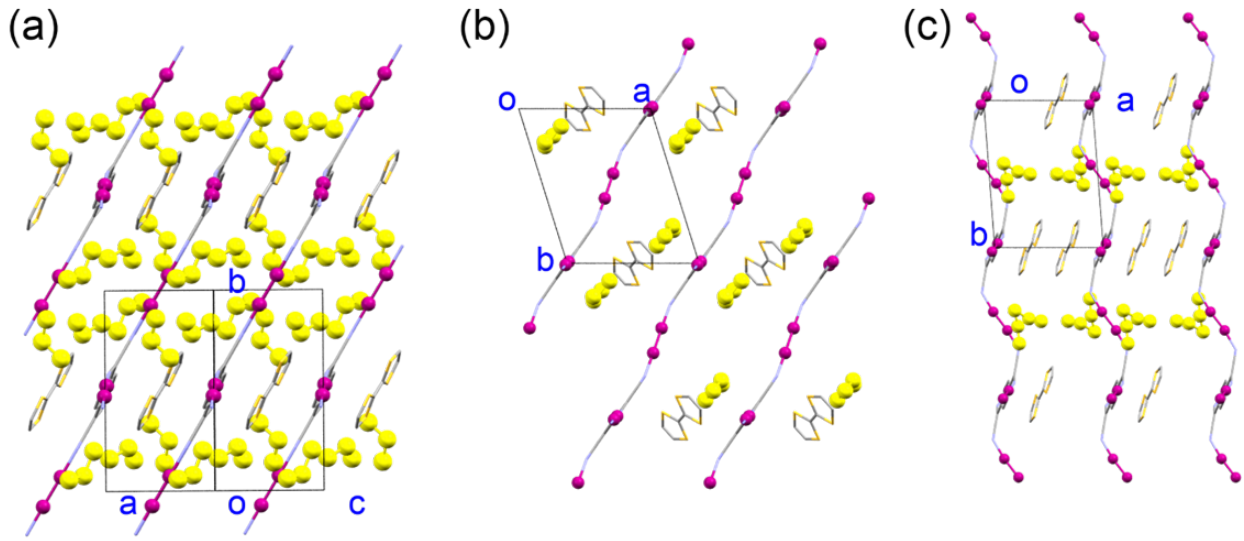

Fig. S1. Packing diagrams for **1** (a), **2** (b) and **3** (c). The solvent molecules are represented by a yellow CPK model. The equatorial carboxylate ligands of the [Rh_2] units and hydrogen atoms are omitted for the sake of clarity.

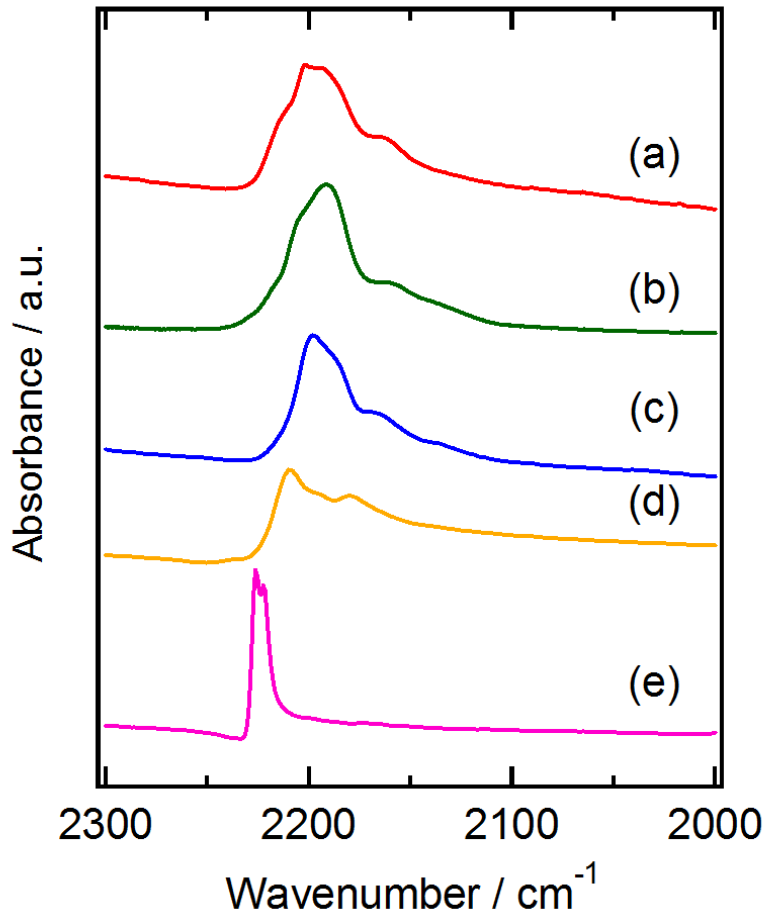

Fig. S2. Infrared spectra in the range 2000–2300 cm^{-1} of **1** (a), **2** (b), **3** (c), $Li^{+}TCNQ^{\bullet-}$ (d) and $TCNQ^{0}$ (e), measured using KBr pellets at room temperature. The observed ν(C≡ N) stretches in **1** – **3** were shifted to lower energies of 2202 cm^{-1}, 2191 cm^{-1} and 2198 cm^{-1} for **1** – **3**, respectively, than the corresponding features in neutral TCNQ, but similar to that in $Li^{+}TCNQ^{\bullet-}$.

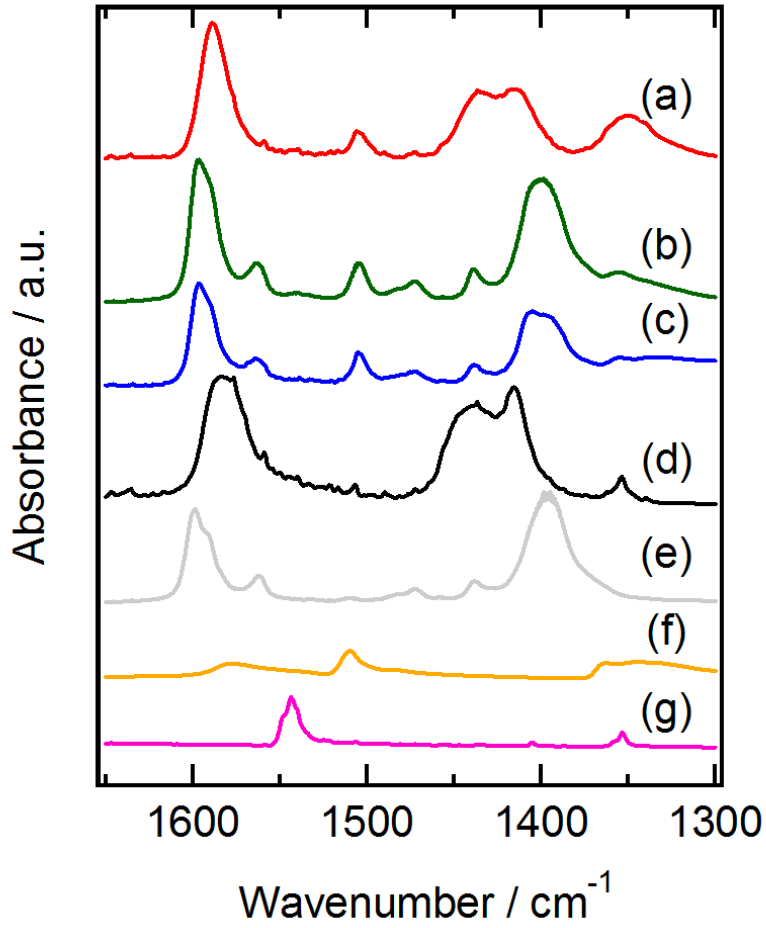

Fig. S3. Infrared spectra in the range 1300-1650 cm^{-1} of (a) **1**, (b) **2**, (c) **3**, (d) $[Rh_2(CH_3CO_2)_4](MeOH)_2$, (e) $[Rh_2(o\text{-}ClPhCO_2)_4](THF)_2$, (f) $Li^{+}TCNQ^{\bullet-}$ and (g) $TCNQ^{0}$, measured using KBr pellets at room temperature.

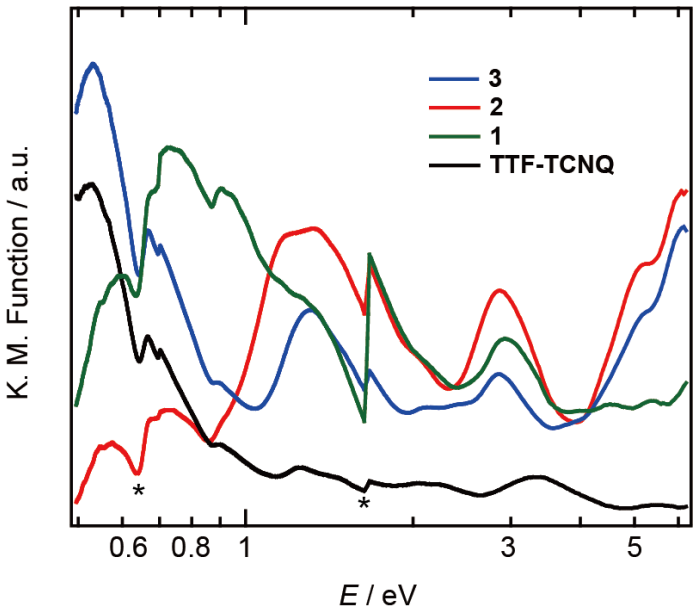

Fig. S4. Absorption spectra of **1**-**3**, and TTF-TCNQ measured on powder pellets diluted with $BaSO_4$ (* indicates nonessential reflection).

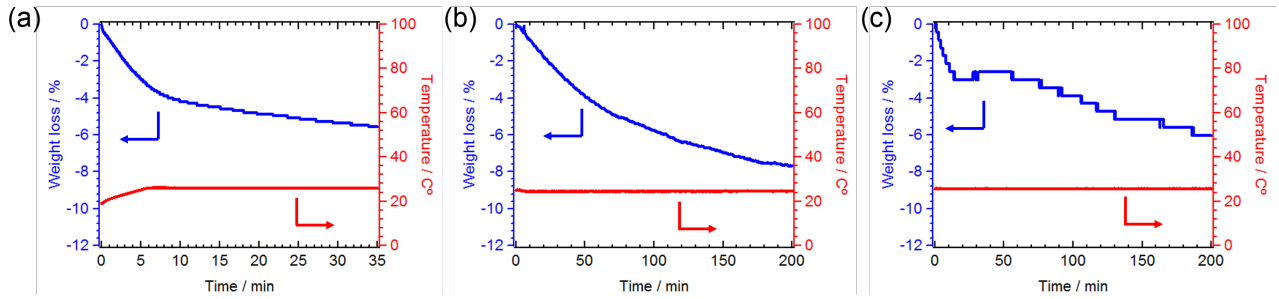

Fig. S5. Time-dependence of TG variation for (a) **1**, (b) **2**, (c) **3**.

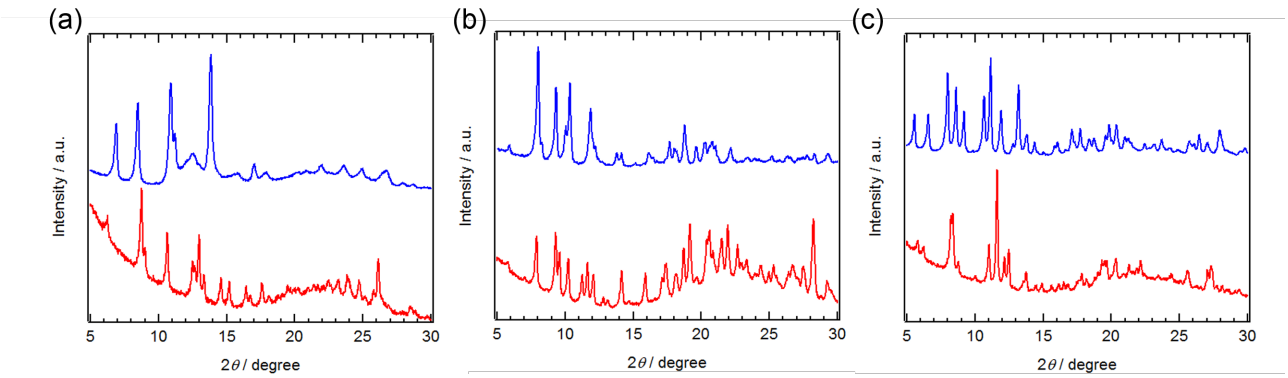

Fig. S6. PXRD patterns of the (a) **1**, (b) **2**, (c) **3** (red) and their solvent-free samples were prepared by evacuating them at room temperature for 48 h, 24 h, and 12 h, respectively.

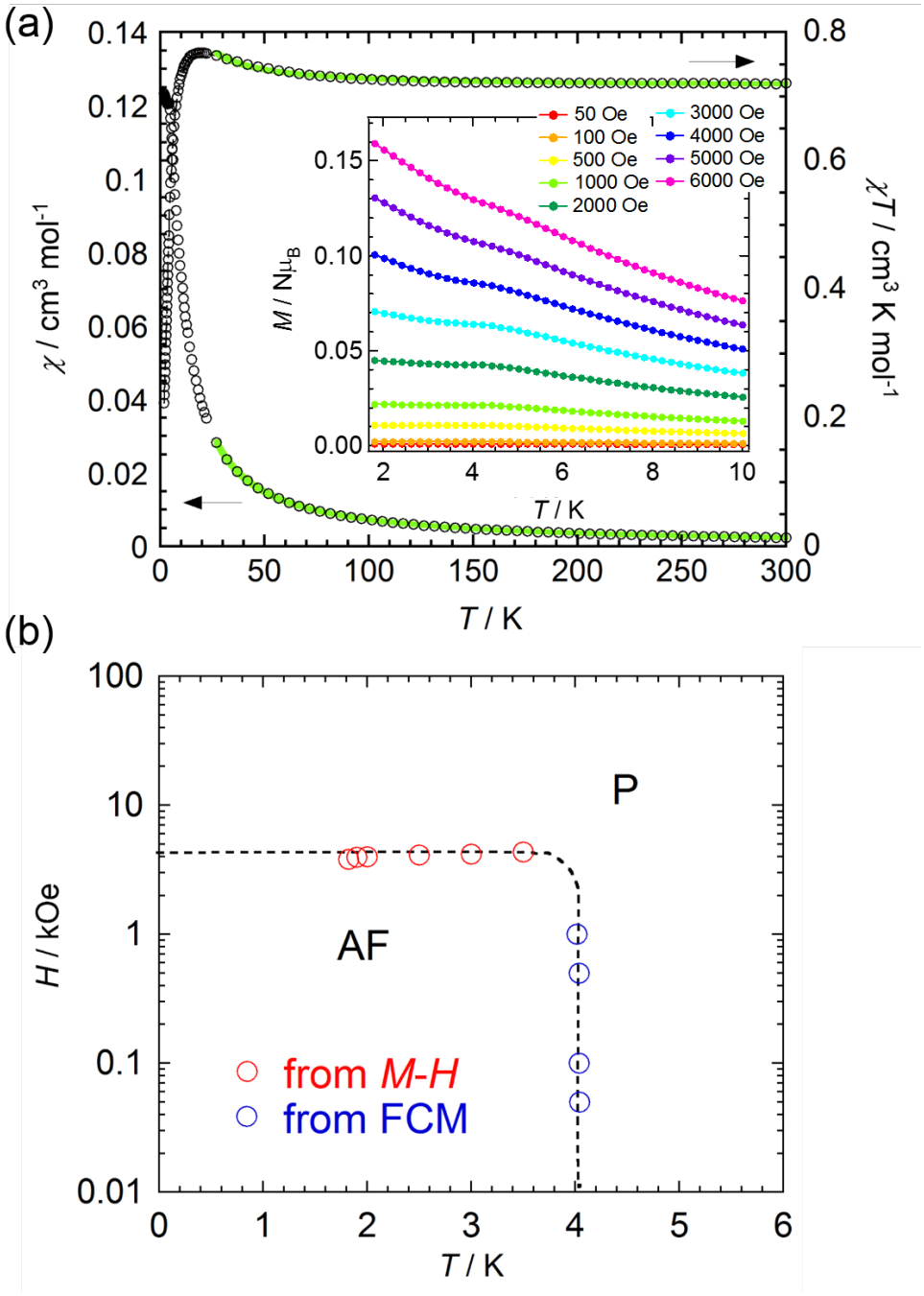

Fig. S7. (a) Temperature dependence of χ and χT of **2** (black), where the green solid line was fitted for the temperature range of 27-300 K using alternating model of Bonner-Fisher. (inset) Field-cooled magnetization curves measured under different external fields for **2**. The solid line is a guide for the eye. (b) *H-T* phase diagram for **2**, where AF and P represent the antiferromagnetic and paramagnetic phases, respectively. The dashed line is a guide for the eye.

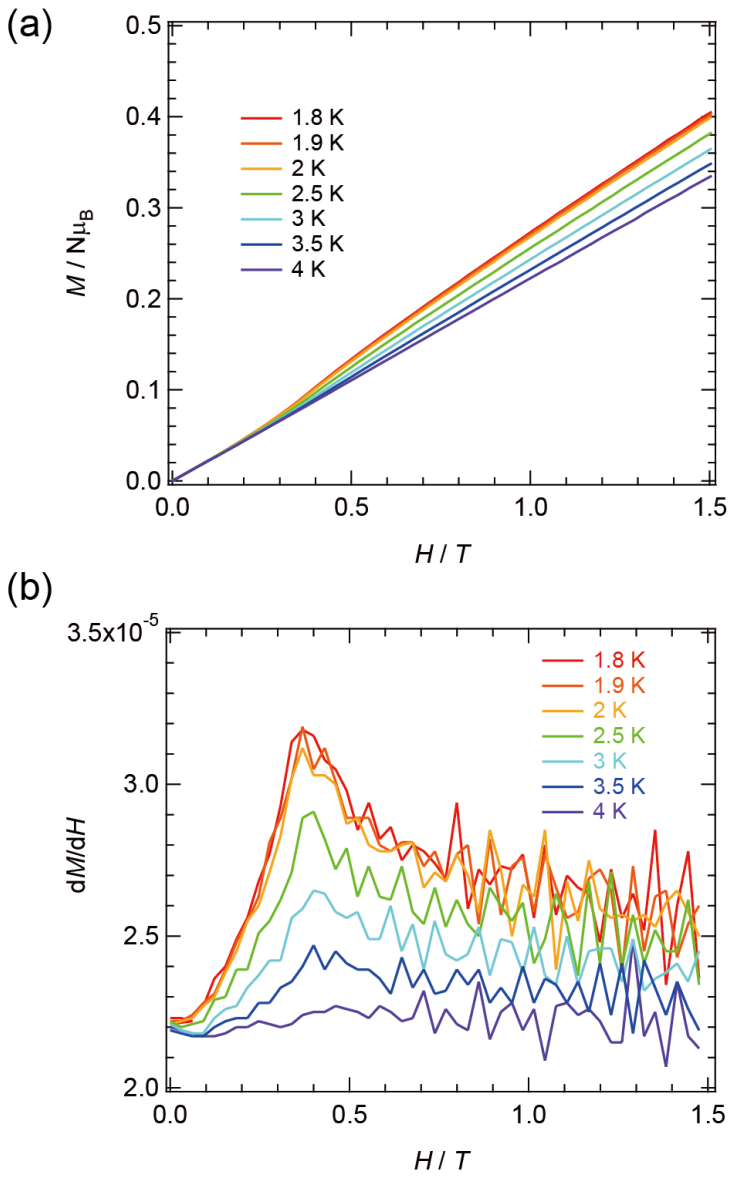

Fig. S8. (a) Field dependence of the magnetization (*M*-*H* plots) for **2**, measured at a range of temperatures, and (b) d*M*/d*H* vs *H* plots for the virgin magnetization of **2**.

References in ESI

1 (a) G. A. Rempel, P. Legzdins, H. Smith, G. Wilikson, *Inorg. Synth.*, **1972**, *13*, 90–91; (b) W. Kosaka, K. Yamagishi, H. Yoshida, R. Matsuda, S. Kitagawa, M. Takata, H. Miyasaka, *Chem. Comm*., **2013**, *49*, 1594–1596; (c) W. Kosaka, K. Yamagishi, A. Hori, H. Sato, R. Matsuda, S.Kitagawa, M. Takata, H. Miyasaka, *J*. *Am*. *Chem*. *Soc*. **2013**, *135*, 18469–18480; (d) Ferraris, J.; Cowan, D. O.; Walatka, V.; Perlstei, J. H., *J*. *Am*. *Chem*. *Soc*. **1973**, *95*, 948–949.

2 G. M. Sheldrick, *SHELEXL 97*, University of Gotingen, Germany, 1997.

3 CrystalStructure 4.0: Crystal Structure Analysis Package, Rigaku Corporation, Tokyo 196-8966, Japan, 2000-2010.

4 Boudreaux, E. A.; Mulay, L. N. *Theory and Applications of Molecular Paramagnetism*, Wiley, New York, **1976**.

5 Long, R. E.; Sparks, R. A.; Trueblood, K. N. *Acta Cryst.* **1965**, *18*, 932–939.

6 Fritche, C. J. Jr.; Arthur, P., Jr. *Acta Cryst*. **1966**, *21*, 139–145.

7 Cooper, W. E.; Kenny, N. C.; Edmonds, J. N.; Nagel, A.; Wudl, F.; Coppens, P. *J. Chem. Soc. Chem. Commum*. **1971**, 889–890.

8 Kistenmacher, T. J.; Phillips, T. E.; Cowan, D. O. *Acta Crystallog*. **1974**, *B30*, 763–768.

9 Yakushi, K.; Nishimura, S.; Sugano, T.; Kuroda, H.; Ikemoto, I. *Acta Crystallogr*. **1980**, *B36*, 358–363.